

Electronic Supplementary Information for

Two sequential enhancements of laser-induced Cu plasma with cylindrical cavity confinement

Ying Wang^{abc}, Anmin Chen^{*abcd}, Laizhi Sui^{ac}, Suyu Li^{ac}, Xiaowei Wang^{ac}, Yuanfei Jiang^{ac}, Xuri Huang^d, Mingxing Jin^{*ac}

^a Institute of Atomic and Molecular Physics, Jilin University, Changchun 130012, China.

^b State Key Laboratory of Laser Propulsion and Application, Equipment Academy, Beijing 101416, China.

^c Jilin Provincial Key Laboratory of Applied Atomic and Molecular Spectroscopy (Jilin University), Changchun 130012, China.

^d Institute of Theoretical Chemistry, Jilin University, Changchun 130012, China.

*Corresponding authors. E-mail: amchen@jlu.edu.cn (Anmin Chen), mxjin@jlu.edu.cn (Mingxing Jin).

This file includes:

- 1. Figure S1:** Schematic diagrams of the experimental setup for optical emission spectroscopy (a) and fast imaging (b).
- 2. Figure S2:** Spectral intensity of plasma emission from Cu with the cylindrical cavity of the diameter = 10 mm and the thickness = 8 mm at three different gains ($g = 2, 8, \text{ and } 40$).
- 3. Figure S3:** Evolution of signal-to-background ratio corresponding to three different gains ($g = 2, 8, \text{ and } 40$).
- 4. Figure S4:** Boltzmann plot obtained from the three Cu (I) lines.
- 5. Figure S5:** Gauss fitting profile of spectral line of Cu (I) transition at 521.82 nm.
- 6. Figure S6:** Temporal evolution of electron density and plasma temperature for laser-induced Cu plasma with the cylindrical cavity of the diameter = 10 mm and the thickness = 8 mm at three different gains ($g = 2, 8, \text{ and } 40$).
- 7. Figure S7:** Evolution of plasma plume. Fast imaging of laser-induced Cu plasma with the spatial confinement by using the cylindrical cavity (diameter = 10 mm, and thickness = 8 mm).
- 8. Figure S8:** Evolution of plasma plume. Fast imaging of laser-induced Cu plasma without the spatial confinement.
- 9. Table S1:** Spectral lines corresponding to the relevant parameters.
- 10. References.**

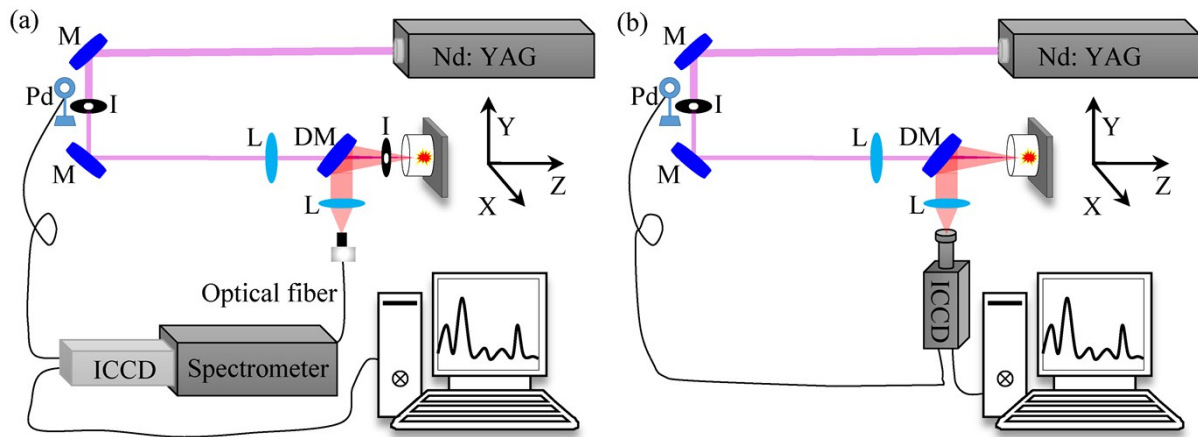


Figure S1 Schematic diagrams of the experimental setup for optical emission spectroscopy (a) and fast imaging (b).

A schematic diagram of the experimental setup for optical emission spectroscopy and fast imaging is shown in Figure S1. For optical emission spectroscopy, the setup has been described in the original paper. For fast imaging, a Nikon camera lens is attached to the ICCD camera (Princeton Instruments, PI-MAX 1024 × 1024), as shown in Figure S1 (b). The images are taken from the top of the plasmas.

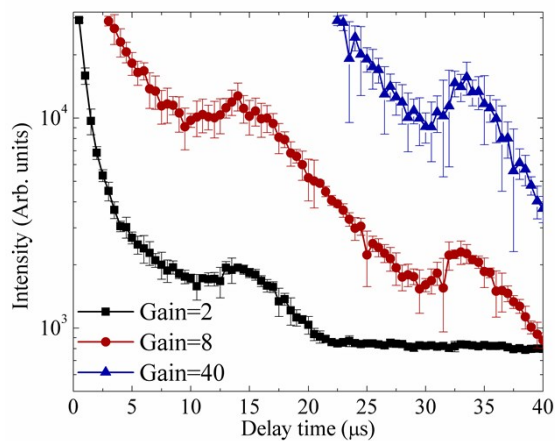


Figure S2 Spectral intensity of plasma emission from Cu with the cylindrical cavity of the diameter = 10 mm and the thickness = 8 mm at three different gains ($g = 2, 8, \text{ and } 40$). The emission line is Cu (I) 510.55 nm. Laser energy is 82 mJ.

The spatial confinement of laser-induced Cu plasmas at different gains is also investigated. Figure S2 shows the temporal evolution of Cu atomic line (510.55 nm) at three different gains ($g = 2, 8, \text{ and } 40$). As can be seen in this figure, the emission intensity is enhanced in the presence of a confinement cavity (diameter = 10 mm, and the thickness = 8 mm) in the range of delay time from 0 μs to 40 μs . As the gain increases, the Cu atomic line emission can be observed more obviously in the time range from 0 μs to 40 μs , especially for the second enhancement.

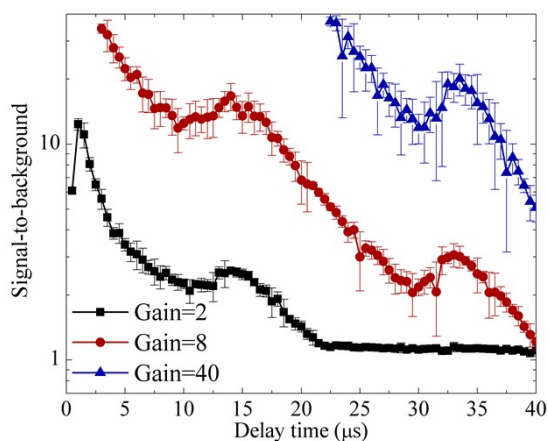


Figure S3 Evolution of signal-to-background ratio corresponding to three different gains ($g=2, 8, \text{ and } 40$).

Laser energy is 82 mJ.

We also calculate the signal-to-background ratio for the selected spectral line with spatial confinement. Figure S3 shows the signal-to-background ratio (S/B) as a function of delay time for Cu (I) line from Figure S2 at three different gains ($g=2, 8, \text{ and } 40$). Similar to the result of time-resolved intensity (Figure S2), there are two enhanced S/B events with spatial confinement. And the signal-to-background ratio is observed more and more obviously with the increase of the gain. The two sequential enhancement events indicate that the measured sensitivity could be improved by using the spatial confinement cavity.

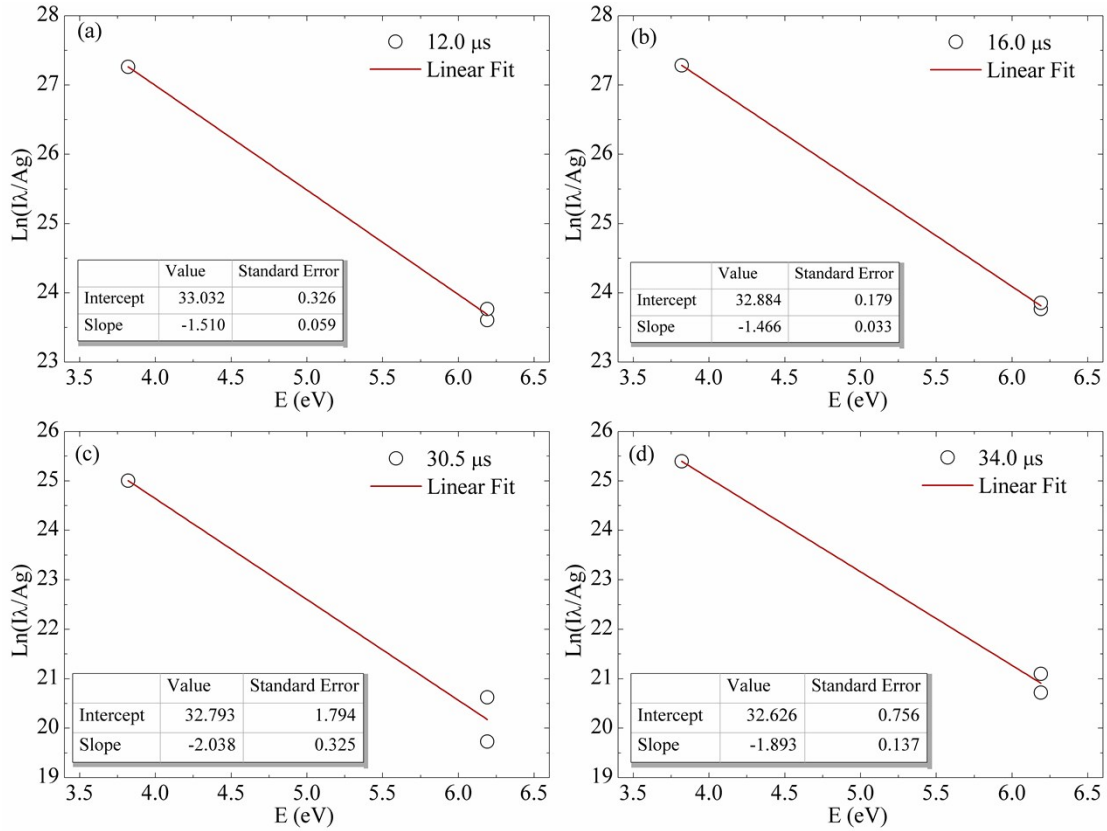


Figure S4 Boltzmann plot obtained from the three Cu (I) lines. Three Cu (I) lines are used to calculate the plasma temperature. The delay times of four plots are 12 μs (a), 16 μs (b), 30.5 μs (c), and 34 μs (d).

The plasma temperature and electron density are two important parameters for describing the plasma characteristics. The plasma excitation temperature is calculated by using the Boltzmann plot method from the relative line intensities of the emission spectra of laser-induced Cu plasma, and the plasma is assumed under the condition of local thermodynamic equilibrium (LTE) and optically thin assumption¹. The equation of plasma excitation temperature can be written as

$$\ln\left(\frac{\lambda I}{g_k A_{ki}}\right) = -\frac{E_k}{k_B T_e} + C \quad (1)$$

Here, λ is the wavelength, I is the intensity of the emission lines, k and i represent the upper and lower atomic levels, g_k is the degeneracy of the upper energy level, A_{ki} is the transmission probability, k_B is the Boltzmann constant, T_e is the plasma temperature, E_k is the energy of the upper level, C is the constant²⁻⁴. In order to

obtain the Boltzmann plot, three spectral lines (510.55 nm, 515.32 nm, and 521.82 nm) are selected to calculate the plasma temperature with a wider range of the upper level energies because these lines are much stronger than the other lines. These spectral parameters can be obtained from a standard spectrum of NIST database and they are listed in Table S1. According to the equation (1), the values of $\ln\left(\frac{I\lambda}{g_k A_{ki}}\right)$ and E_k are calculated, to obtain the plasma temperature, we need to achieve the slope of the function $(-1/k_B T)$ by using the linear fit of data points. The Boltzmann plot and the slope value are shown in Figure S4. The selected typical delay times are 12.0 μs (a), 16.0 μs (b), 30.5 μs (c), and 34.0 μs (d), respectively. Finally, the temperature T_e is calculated through the slope value.

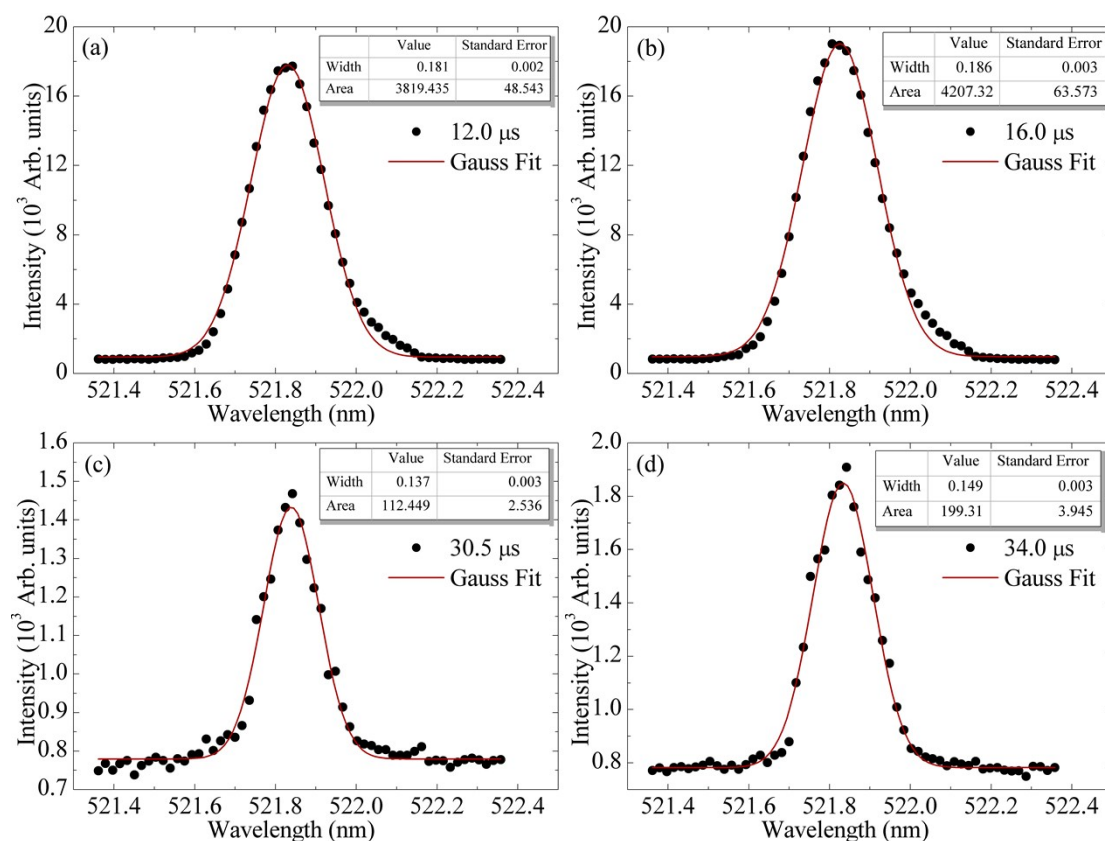


Figure S5 Gauss fitting profile of the spectral line of Cu (I) transition at 521.82 nm. The delay times of four spectral lines are 12.0 μs (a), 16.0 μs (b), 30.5 μs (c), and 34 μs (d), respectively.

Electron density is determined by FWHM of spectral line according to the Stark broadened line profile⁵⁻⁶.

It can be expressed as follows⁷:

$$\Delta\lambda_{1/2} = 2\omega \frac{N_e}{10^{16}} \quad (2)$$

where $\Delta\lambda_{1/2}$ is the FWHM of spectral lines, ω is the electron impact parameter (2.2 Å) and N_e is the electron number density^{2, 8}. The Cu I line (521.82 nm) is used to calculate the electron density. Figure S5 shows the typical Gauss fitting profile of Cu (I) at different delay times (12.0 μs, 16.0 μs, 30.5 μs, and 34.0 μs).

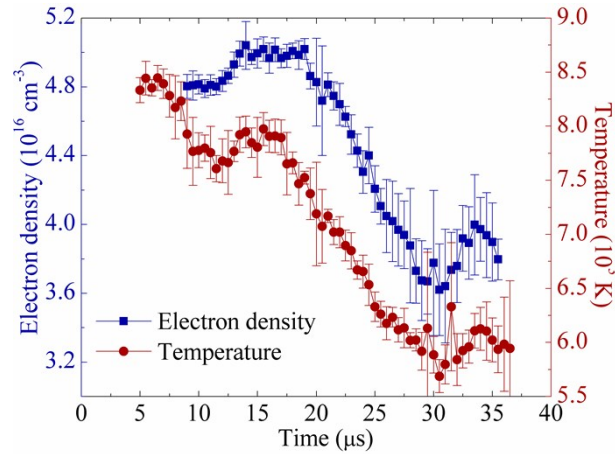


Figure S6 Temporal evolution of electron density and plasma temperature for laser-induced Cu plasma with the cylindrical cavity of the diameter = 10 mm and the thickness = 8 mm at three different gains ($g = 2, 8,$ and 40). Laser energy is 82 mJ.

Figure S6 shows the electron density and plasma temperature as a function of delay time using the spatial confinement cavity. In Figure S6, the electron density of plasma is in the range from $3.6 \times 10^{16} \text{ cm}^{-3}$ to $5.0 \times 10^{16} \text{ cm}^{-3}$, the plasma temperature is in the range from 5500 K to 8500 K. And the change of electron density is similar to the change of plasma temperature. There are two obvious fluctuations during the processes of plasma expansion, ie, the first enhancement (delay time is 16 μs) and the second enhancement (delay time is 34 μs). The delay times of two spectral enhancements in Figure S2 are in agreement with the delay times of the extremes of electron density and plasma temperature. That is to say, two enhancement events of Cu atomic emission lines are attributed to the compressed plasma with higher plasma temperature and bigger particle

density by reflected shockwave.

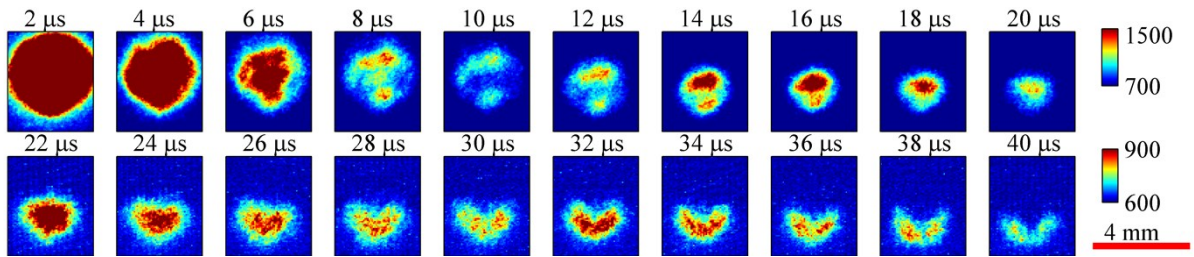


Figure S7 Evolution of plasma plume. Fast imaging of laser-induced Cu plasma with the spatial confinement by using the cylindrical cavity (diameter = 10 mm, and thickness = 8 mm). Laser energy is 82 mJ. For the top row (2 μ s – 20 μ s), the scale is from 700 to 1500. For the bottom row (22 μ s – 40 μ s), the scale is from 600 to 900.

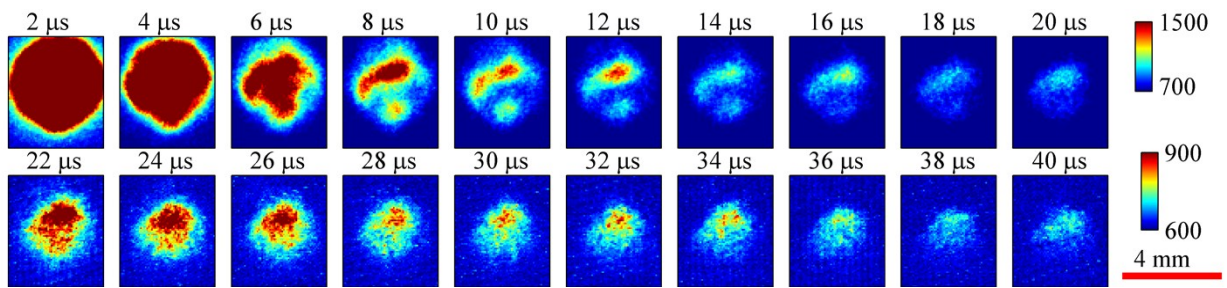


Figure S8 Evolution of plasma plume. Fast imaging of laser-induced Cu plasma without the spatial confinement. Laser energy is 82 mJ. For the top row (2 μ s – 20 μ s), the scale is from 700 to 1500. For the bottom row (22 μ s – 40 μ s), the scale is from 600 to 900.

To study the intensity of the plasma plumes with spatial confinement, fast imaging is employed. The expansion of laser-induced Cu plasma obtained by ICCD camera can be observed in Figure S7. Each image is obtained from a single laser shot. As it can be seen from these images, at the top row, it appears the first enhancement in the delay time range of 14 μ s – 18 μ s, at the bottom row, it appears the second enhancement in the delay time range of 32 μ s – 36 μ s. This is also consistent with the delay time of the spectral enhancement in Figure S2. However, the enhanced emission of plasma plume can not be observed in Figure S8.

Table S1 Spectral lines corresponding to the relevant parameters. They are used to calculate plasma temperature.

Wavelength λ (nm)	Transition	Upper-level energy E_i (eV)	Upper-level degeneracy g_i \times Transition probability A_{ij} (10^8 s^{-1})
510.55	$3d^9 4s^2 - 3d^{10} 4p$	3.81	0.08
515.32	$3d^{10} 4p - 3d^{10} 4d$	6.19	2.40
521.82	$3d^{10} 4p - 3d^{10} 4d$	6.19	4.50

References

1. H. Shakeel, M. Mumtaz, S. Shahzada, A. Nadeem and S. Haq, *Plasma Sources Science and Technology*, 2014, **23**, 035006.
2. S. Bashir, N. Farid, K. Mahmood and M. S. Rafique, *Applied Physics A*, 2012, **107**, 203-212.
3. J. Chen, Z. Chen, J. Sun, X. Li, Z. Deng and Y. Wang, *Applied Optics*, 2012, **51**, 8141-8146.
4. A. Nakimana, H. Tao, X. Gao, Z. Hao and J. Lin, *Journal of Physics D: Applied Physics*, 2013, **46**, 285204.
5. H. Hegazy, E. A. Abdel-Wahab, F. M. Abdel-Rahim, S. H. Allam and A. E. M. Nossair, *The European Physical Journal D*, 2014, **68**, 1-8.
6. S. Jie, Y. Zhengcai, L. Xiaoliang, S. Yanchao, Z. Peixi, S. Shaohua and H. Bitao, *Plasma Science and Technology*, 2015, **17**, 147.
7. W. Jingge, F. Hongbo, N. Zhibo, C. Xinglong, H. Wengan and D. Fengzhong, *Plasma Science and Technology*, 2015, **17**, 649.
8. X.-F. Li, W.-D. Zhou and Z.-F. Cui, *Frontiers of Physics*, 2012, **7**, 721-727.